Environmental Science & Technology

pubs.acs.org/est

Article

Photogranulation in a Hydrostatic Environment Occurs with Limitation of Iron

Abeera A. Ansari, Arfa A. Ansari, Ahmed S. Abouhend, Joseph G. Gikonyo, and Chul Park*

Cite This: *Environ. Sci. Technol.* 2021, 55, 10672−10683

Read Online

ACCESS | Metrics & More | Article Recommendations | Supporting Information

ABSTRACT: Filamentous cyanobacteria are an essential element of oxygenic photogranules for granule-based wastewater treatment with photosynthetic aeration. Currently, mechanisms for the selection of this microbial group and their development in the granular structure are not well understood. Here, we studied the characteristics and fate of iron in photogranulation that proceeds in a hydrostatic environment with an activated sludge (AS) inoculum. We found that the level of Fe in bulk liquids (Fe_{BL}) sharply increased due to the decay of the inoculum but quickly diminished along with the bloom of microalgae and the advent of the oxic environment. Iron linked with extracellular polymeric substances (Fe_{EPS}) continued to decline but reached steady low values, which occurred along with the appearance of granular structure. Strong negative correlations were found between Fe_{EPS} and the pigments specific for cyanobacteria. Spectroscopies revealed the presence of amorphous ferric oxides in pellet biomass, which seemed to remain unaltered during the photogranulation process. These results suggest that the availability of Fe_{EPS} in AS inoculums—after algal bloom—selects cyanobacteria, and the limitation of this Fe pool becomes an important driver for cyanobacteria to granulate in a hydrostatic environment. We therefore propose that the availability of iron has a strong influence on the photogranulation process.

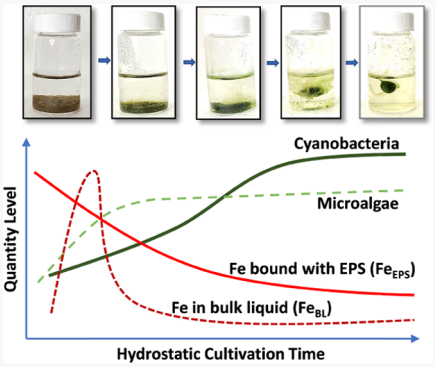

KEYWORDS: *OPG, hydrostatic cultivation, activated sludge inoculum, filamentous cyanobacteria, EPS, wastewater treatment, photosynthetic aeration*

INTRODUCTION

Iron (Fe) is an essential micronutrient for living organisms. It is a critical element in numerous cellular processes, including respiration, pigment synthesis, nitrogen assimilation, nitrogen fixation, and photosynthesis.[1−3] In the photic zones of aquatic environments, Fe is known to limit the productivity of primary producers and affect biosynthesis of metabolites, which can induce physiological changes in cells.[1,4−6]

Phototrophic prokaryote, cyanobacteria, require high-level Fe compared to eukaryotic microalgae and heterotrophic bacteria due to their Fe-rich photosynthetic apparatuses.[3,7−10,76] To meet their Fe requirements and compete against other phototrophic microbes, cyanobacteria exhibit multiple Fe uptake mechanisms, including the Fe reductive mechanism[5,11−16] and siderophore-based mechanism.[17,18] Siderophores are low-molecular-weight extracellular Fe(III) chelators, which scavenge and transport Fe into cells.[17,18] Using these siderophores, cyanobacteria can also thrive in Fe-limited environments unlike microalgae.

Cyanobacteria can undergo numerous physiological adaptations to Fe limitation in oxic environments. An example is substituting ferredoxin, an Fe-containing electron-transfer protein, with Fe-free flavodoxin.[19] It has also been shown that *Trichodesmium* N_2-fixing marine filamentous cyanobacteria, aggregate to form puff or tuft-like colonies under Fe limitation.[20−22] These *Trichodesmium* colonies are known to host heterotrophic bacterial community (i.e., bacterial epibionts of *Trichodesmium* holobiont) and via their tightly regulated relationship utilize dust-driven or mineral Fe from the environment.[23−25]

Sphere-like aggregation of filamentous cyanobacteria has been observed in different environments. Oxygenic photogranules (OPGs) are dense microbial aggregates growing in wastewater systems, consisting of mat-like layers of filamentous cyanobacteria that enclose microalgae and heterotrophic bacteria in spherical structures.[26,27] OPGs can be produced by incubating activated sludge (AS) in a hydrostatic environment under illumination.[26] These hydrostatically produced OPGs are used as seed for bioreactors, treating wastewater without aeration,[26,28,29] which currently causes the highest energy demand in wastewater systems.

Studies concurrently reported that in hydrostatic cultivation of OPGs, unicellular and filamentous green algae make early

Received: October 31, 2020
Revised: July 1, 2021
Accepted: July 2, 2021
Published: July 13, 2021

https://doi.org/10.1021/acs.est.0c07374
Environ. Sci. Technol. 2021, 55, 10672−10683

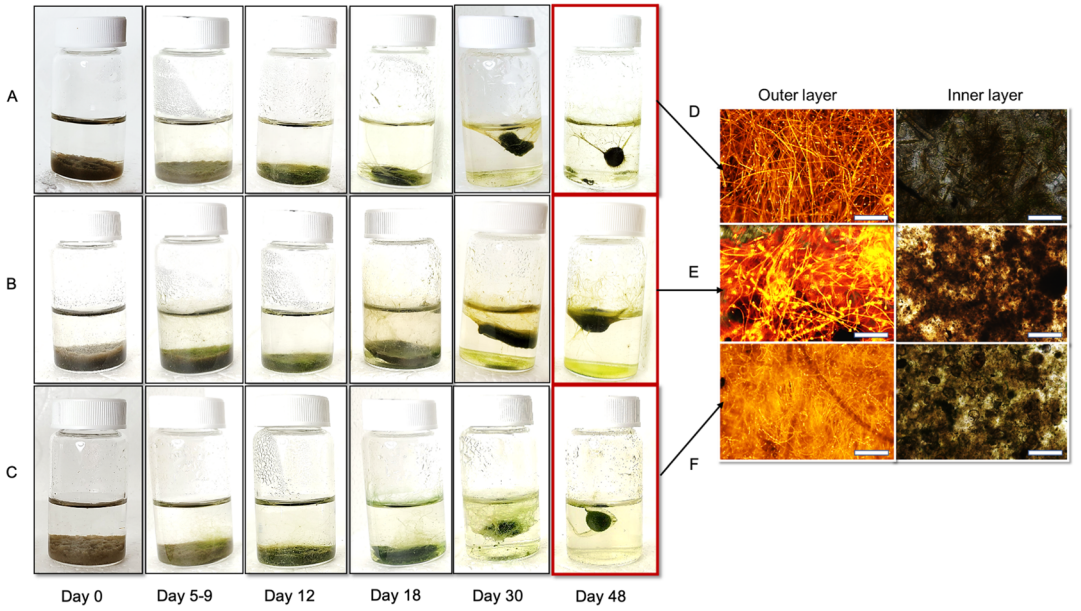

Figure 1. Progression of photogranulation under hydrostatic conditions. Cultivation inoculums: AS from the aeration basin of (A) Amherst, (B) Hadley, and (C) Springfield WWTPs. (D−F) Show microscopic images of outer layers (autofluorescence microscopy) and inner biomass (brightfield microscopy) of mature photogranules produced from Amherst, Hadley, and Springfield AS, respectively. Scale bars in all microscopic images are 400 μm.

bloom, followed by a substantial growth of filamentous cyanobacteria.[26,27,29,30] Milferstedt et al.[26] reported that the order Oscillatoriales in Cyanobacteria, also known as the subsection III cyanobacteria,[31] get enriched in OPGs regardless of the source of AS inoculum. Selection of Oscillatoriales after algal bloom was linked with their ability to utilize organic nitrogen following early depletion of dissolved inorganic nitrogen (DIN).[27,30] Nevertheless, the main granulation phase was observed to occur when cyanobacterial growth reached steady state,[27] implying that nutrient limitation and stasis in filamentous cyanobacteria are requisite for granulation. In this aspect, some cultivations that produced granules still contained dissolved nitrogen, including nitrate (resulting from nitrification occurring in cultivation) and organic nitrogen, as well as phosphate and dissolved carbon when granulation occurred.[27,30] These studies, therefore, suggest that there are some other resource limitations, which could have stopped cyanobacterial growth and promoted granulation.

Considering the significance of Fe in cyanobacterial growth and their physiology, we hypothesize that the availability of Fe has significant influence on the selection of cyanobacteria, and its limitation has impact on the formation of spherical OPGs. To examine the hypothesis, we investigated the characteristics and fate of Fe during the transformation of AS inoculums into OPGs in hydrostatic cultivations. We determined the quantity and oxidation state of Fe in bulk liquids and also traced Fe that is associated with extracellular polymeric substances (EPSs). Various spectroscopies were employed to explore the fate of crystalline and amorphous Fe in AS inoculums in photogranulation. The results of this study are expected to provide insights on the photogranulation phenomenon, which is the principle of a new granular process developed for aeration-free wastewater treatment.

MATERIALS AND METHODS

Detailed methods are provided in the Supporting Information.

Hydrostatic Cultivation of Oxygenic Photogranules. AS was collected from the aeration basins of three local wastewater treatment plants (WWTP) in Amherst, Hadley, and Springfield, MA, USA. 10 mL of AS was pipetted into 20 mL glass vials and capped. These vials were then incubated hydrostatically for the course of 48 days under continuous illumination of 18−45 μmol/m^2 s. Illumination was provided via LED having natural daylight spectrum (4200K). Incubation was conducted at 22 °C in a temperature-controlled room.

Fe in Different Fractions of Biomass. Fe in bulk liquid (Fe_{BL}), Fe linked with EPS (Fe_{EPS}), and Fe in whole biomass (Fe_{whole}) were determined periodically over the cultivation period. Fe_{BL} was analyzed for two size fractions: colloidal (0.45 μm—30 kDa) and dissolved (<30 kDa)[32] fractions. Filtration of bulk liquid was conducted inside a glovebox with continuous N_2 purging to avoid the oxidation of Fe. The filtrates were acidified with conc. trace-metal grade HNO_3 (2% by vol) and stored at 4 °C till analysis. Fe_{EPS} is defined to be Fe present in the EPS extract, which was obtained via sequential extraction of sonication and base treatment of biomass.[29,33] For this fraction of Fe, the filtered EPS extracts were acidified with the abovementioned HNO_3 and stored at 4 °C. Fe_{whole} was determined after subjecting the whole samples to acid digestion.[34] The acid-digested samples were filtered through a filter paper and stored at 4 °C till further analysis. The total Fe concentration in these samples was quantified using inductively coupled plasma mass spectrometry (PerkinElmer SCIEX). The pellet Fe (Fe in pellet, Fe_{pellet}) was calculated by subtracting Fe_{EPS} and Fe_{BL} (<0.45 μm) from Fe_{whole}.

Speciation of Fe. The oxidation state of Fe_{BL} was determined as Fe(II) and Fe(III) using the Ferrozine reagent method.[35] Three spectroscopic techniques of electron paramagnetic resonance (EPR), powder X-ray diffraction (PXRD), and Fourier transform infrared (FTIR) were performed on vacuum dried, powdered whole biomass samples. EPR was used to identify the species of ferric iron. Its measurements were carried out on a Bruker Elexsys-500 fitted with super high

https://doi.org/10.1021/acs.est.0c07374
Environ. Sci. Technol. 2021, 55, 10672−10683

QE X-band cavity. PXRD was employed to distinguish between crystalline and amorphous Fe as well as for the identification of crystalline Fe. PXRD patterns were collected on a Rigaku Smart Lab SE using Bragg−Brentano configuration and Cu K-source. FTIR was utilized for functional group and surface chemistry analysis and was carried out on a Bruker Alpha-P FTIR spectrometer equipped with an attenuated total reflectance platinum diamond optic.

Analytical Measurements. Total and volatile suspended solids (VSS) and chlorophyll content were determined using the Standard Methods.[36] The levels of phycobilin, accessory pigments of cyanobacteria, in biomass were determined with modification of the methods of Bennett and Bogorad[37] and Islam and Beardall.[38] Background interference for phycobilin quantification was removed using the approach by Lauceri et al.[39] Polysaccharide in bulk-liquid fractions and EPS was measured using the phenol-sulfuric method[40] with glucose as standard. Protein was measured using the modified Lowry method[41] with bovine serum albumin as standard. Dissolved total nitrogen (DTN) and dissolved organic carbon (DOC) in filtered bulk-liquid fractions (0.45 μm and 30 kDa) were determined using a TOC/TN analyzer. DIN (NO_2^-, NO_3^-, and NH_4^+), SO_4^{2-}, and PO_4^{3-} in 0.45 μm filtrates were determined using a Metrohm 850 Professional Ion Chromatograph. Dissolved organic nitrogen (DON) was obtained by subtracting DIN from DTN. Dissolved oxygen (DO) was measured using a potable DO probe (Orion star A223, Thermo Scientific) inside the glovebox under continuous N_2 purge.

Microscopy. We used both brightfield and autofluorescence microscopy to study shift in microbial community and structural development during the progression of photogranulation. Red fluorescence protein excitation (530 nm) was used to detect the presence of filamentous cyanobacteria which produced golden-orange fluorescence as an indicator of phycobilin pigment phycoerythrin.[42]

Statistical Analysis. The Pearson correlation coefficient (r) was determined to assess correlations among variables. The two-sample t-test ($\alpha = 0.05$) was also performed to determine the statistical significance between variables (p-value).

RESULTS

Progression of Photogranulation under Hydrostatic Conditions. The hydrostatic cultivations with three AS sources exhibited similar progression of photogranulation (Figure 1). After about 4 days of incubation, green layers started to develop on settled sludge biomass, which included unicellular and filamentous green algae (Figure S1A−F). Motile filamentous cyanobacteria made first clear appearance, as observed by microscopy around day 9−12 (Figure S1G−I). Cyanobacterial growth continued in the top green layers during day 15−18 (Figure S1J−L). By day 18, cyanobacteria became a dominant phototrophic community in the outer layer, which eventually surrounded the settled biomass, thereby molding it into a mat-like structure (Figure 1). Between days 18 and 30, both macro- and microscopic observations revealed extensive amounts of slime-like matter, which seemed to promote biomass contraction and floatation. During these periods, both Amherst and Springfield sets showed significant biomass contraction, whereas the Hadley set showed slower changes. The appearance of mature sphere-like OPGs followed this stage in each cultivation. The produced OPGs consisted of an outer layer of motile filamentous cyanobacteria, enclosing aggregates of bacteria, unicellular and filamentous microalgae, other protist organisms, including *Arcella*, and minerals (Figure 1D−F).

Consistent with microscopy, all cultivations showed substantial increases in chlorophyll *a*, the essential pigment for oxygenic phototrophic organisms (Figure S2A). Chlorophyll *b* and chlorophyll *c*, which have been used as a surrogate for green algae and diatoms in OPGs, respectively,[43−45] generally increased until day 12 after which they either leveled off or decreased (Figure S2B,C). In contrast to chlorophylls *b* and *c*, phycobilin, essential accessory pigments in cyanobacteria,[43] continued to increase till much later periods (Figure S2D). Positive correlations existed between phycobilin and chlorophyll *a* for Amherst ($r = 0.94$), followed by Hadley ($r = 0.79$) and Springfield ($r = 0.70$) cultivations (Table S1). Considerably weaker correlations were found between phycobilin and both chlorophylls *b* and *c*, especially for Amherst and Hadley cultivations (Table S1). Despite these significant increases in phototrophic biomass, the change in the total biomass concentration as VSS was less than 9 ± 4% (data not shown), congruent with earlier reports,[26,27,30] indicates recycling of carbon and nutrients within this closed cultivation.

Fate of Dissolved Macronutrients in Hydrostatic Cultivation. The significant release of phosphate within less than 4 days was evident for all three cultivations (Figure 2A), indicating the decay of cells from AS inoculum under anaerobic conditions. After this initial release, both Amherst and Springfield sets showed substantive removal of PO_4^{3-}, but this was quickly followed by additional major release. Although further removal occurred later, significant levels of PO_4^{3-} remained in both cultivations. In the Hadley set, on the other hand, the released PO_4^{3-} got nearly depleted, indicating the development of P-limited condition in this cultivation.

The release of ammonia for the first 4 days, especially in Hadley and Springfield sets, concurs with the initial release of PO_4^{3-}. Nearly all ammonia in Amherst and Springfield sets was removed by day 6. Ammonia remained undetected for the remaining cultivation periods. Depletion of ammonia was also the case for the Hadley set although it took longer likely due to greater amounts of ammonia initially present and released during the early period. For nitrate, initial nitrate in all three inoculums was quickly consumed and remained either at very low level or depleted throughout the cultivations. One time release of nitrate in the Springfield set indicates nitrification. This was also observed in Kuo-Dahab et al.[27] with Amherst AS inoculum; in this study, however, the level of nitrate kept increasing along with production of spherical OPGs.

In addition to inorganic species, the fate of DOC and DON was also investigated (Figure S3). Both DOC and DON increased from the dissolved fraction of bulk liquid (<30 kDa) during the course of photogranulation for all three cultivations. The increase in DOC and DON accompanying the photogranulation in hydrostatic cultivation was also reported earlier.[27]

Dynamics of Iron in Bulk-Liquid Fractions. The bulk-liquid Fe (Fe_{BL}) in three AS inoculums was, on average, 0.37 ± 0.16 mg/L and existed primarily in the dissolved fraction (<30 kDa): Amherst, 88%; Hadley, 92%; and Springfield, 67% (Figure 3). As cultivation proceeded, there was a sharp increase in Fe_{BL}, both in dissolved and colloidal fractions, by day 2. Both dissolved and colloidal Fe then quickly declined and reached steady points after day 12. The level of dissolved Fe became once again greater than colloidal Fe in all bulk

https://doi.org/10.1021/acs.est.0c07374
Environ. Sci. Technol. 2021, 55, 10672−10683

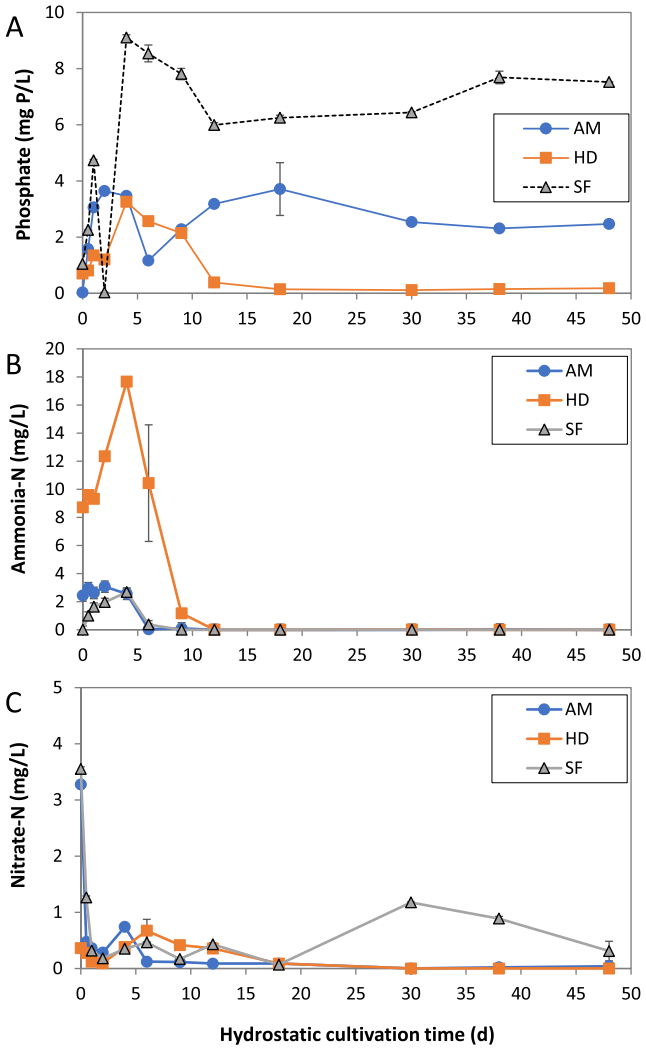

Figure 2. Fate of DIN and phosphate in hydrostatic cultivation of OPGs with AS inoculums from three sources. (A) Phosphate, (B) ammonia, and (C) nitrate. Nitrite was mostly undetected throughout the cultivation period. AM: Amherst cultivation; HD: Hadley cultivation; SF: Springfield cultivation. Error bars represent the range of results from duplicate cultivation samples.

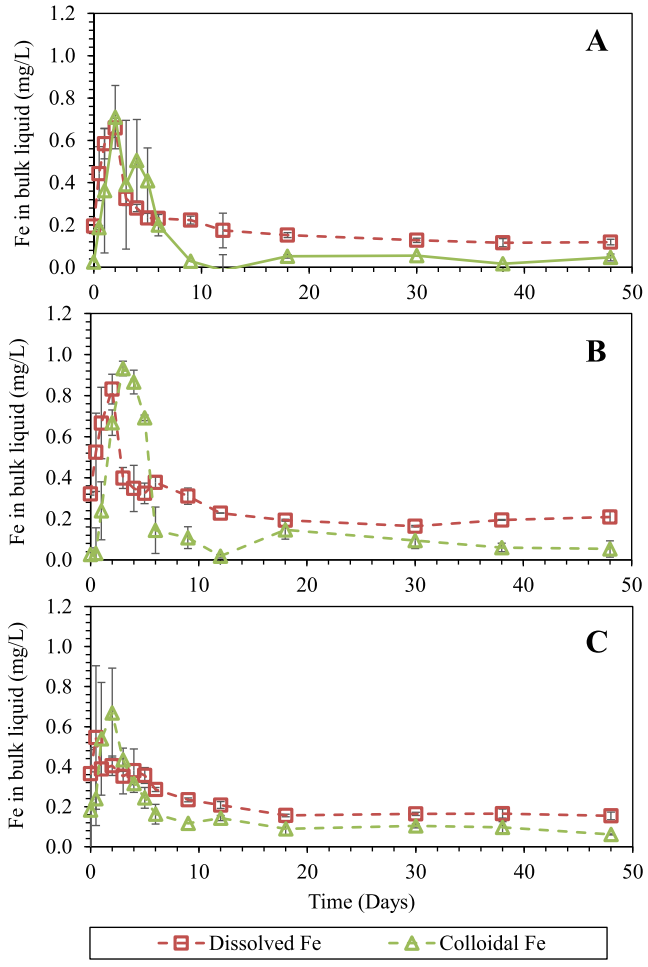

Figure 3. Dynamics of dissolved Fe and colloidal Fe in bulk liquids in hydrostatic cultivation of photogranules with AS from (A) Amherst, (B) Hadley, and (C) Springfield WWTPs. Error bars represent the standard deviation from triplicate samples.

liquids, which was statistically significant (Amherst, $p < 0.0004$; Hadley, $p < 0.0025$; and Springfield, $p < 0.0032$).

Iron released into bulk liquids by day 2 consisted of both ferric iron and ferrous iron (Figure 4A,B). The total Fe release contained an average of 36, 54, and 36% Fe(II) in Amherst, Hadley, and Springfield, respectively. During this time period, DO became depleted (Figure 4C). The development of anaerobic conditions should have accounted for the reduction of a fraction of Fe(III) in AS into Fe(II) and its release into the bulk liquid. Photochemical reduction of Fe might have also occurred under illumination,[2] thereby contributing to the release of Fe(II) into bulk liquid. Both dissolved and colloidal Fe(II) decreased after day 2, ultimately becoming undetectable after day 9−12. The Fe(III) fractions also showed decrease from day 3 to 9 (Figure 4B); however, in contrast to Fe(II), Fe(III) remained in bulk liquids with steady values for the reminder of cultivation period. The depletion of Fe(II) occurred simultaneously with an increase in DO. Fe(II) is the most preferred form of Fe for phototrophic growth, and it is also thermodynamically unstable in the presence of oxygen, rapidly converting into Fe(III).[6,46,47] This suggests that the growth of phototrophic community influenced the Fe oxidation states in bulk liquid during the progression of photogranulation.

Table 1 shows correlations of Fe_{BL} with dissolved nutrients and the biomass' photosynthetic pigments. Fe_{BL}, either as the total or as a size fraction, showed moderate to strong positive correlations with NH_4^+ across the cultivations. This NH_4^+ is likely originated from the degradation of protein in AS inoculum, which was demonstrated for high affinity for Fe(III).[48−51] Hence, as Fe(III) is reduced by anaerobic conditions and by photochemical reactions, proteins bound with Fe(III) could have undergone hydrolysis and degradation, leading to the production of NH_4^+. In Amherst cultivation, the correlations of NH_4^+ with colloidal and dissolved Fe were rather similar, whereas in Hadley and Springfield sets, the correlations were much stronger for dissolved Fe than colloidal Fe. For phosphate, only Hadley set showed a meaningful correlation with Fe_{BL}. Both nitrate and sulfate overall exhibited no significant correlations with Fe_{BL}. DOC in a 30 kDa filtrate exhibited moderate negative correlations with dissolved Fe pool (Table S2). DON showed no significant correlation with Fe_{BL} except for the Amherst set in which clear negative correlations existed between colloidal DON and both colloidal and dissolved Fe in bulk liquid.

https://doi.org/10.1021/acs.est.0c07374
Environ. Sci. Technol. 2021, 55, 10672−10683

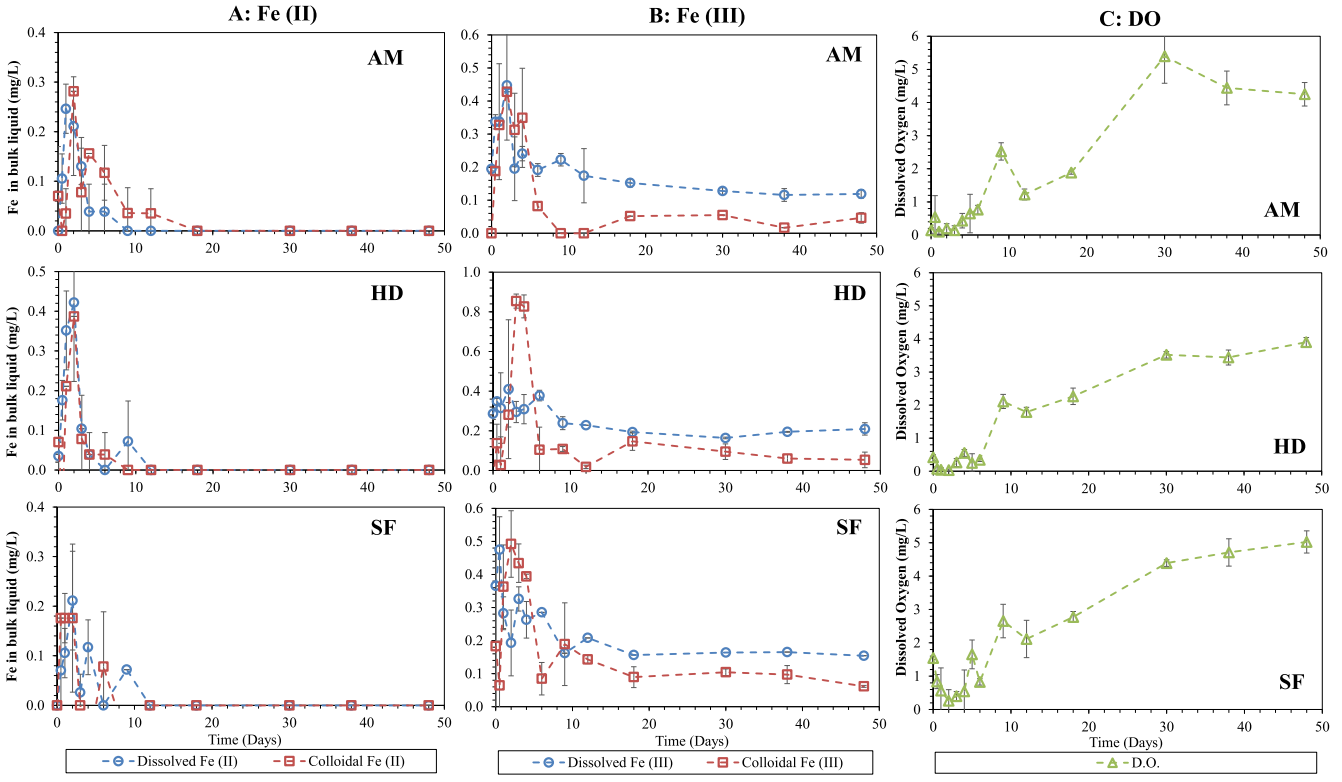

Figure 4. Dynamics of dissolved Fe(II,III) and colloidal Fe(II,III) as well as DO during the photogranulation process. Figures in column (A) Fe(II); column (B) Fe(III); and column (C) DO. AM: Amherst cultivation; HD: Hadley cultivation; SF: Springfield cultivation. Error bars represent the range of results from duplicate cultivation samples.

Table 1. Pearson Correlation Coefficients of Colloidal Fe and Dissolved Fe in Bulk Liquid with Dissolved Inorganic Nutrients and Photosynthetic Pigments Produced During the Cultivation of Photogranules in a Hydrostatic Environment[a]

	Amherst		Hadley		Springfield	
	colloidal Fe	dissolved Fe	colloidal Fe	dissolved Fe	colloidal Fe	dissolved Fe
	30 kDa < Fe < 0.45 μm	Fe < 30 kDa	30 kDa < Fe < 0.45 μm	Fe < 30 kDa	30 kDa < Fe < 0.45 μm	Fe < 30 kDa
NH_4^+	**0.86**	**0.70**	0.15	0.66	0.24	**0.77**
	0.68	0.62	0.13	0.55	−0.25	**0.94**
	0.86	**0.72**	0.11	**0.72**	0.47	0.17
NO_3^-	0.24	−0.04	−0.12	0.0.3	0.02	0.31
	0.31	−0.12	0.18	−0.19	−0.44	−0.24
	0.18	0.02	−0.23	0.44	0.48	0.69
PO_4^{3-}	0.05	0.24	**0.84**	0.26	−0.21	−0.48
	−0.25	0.20	0.49	0.09	−0.33	−0.36
	0.20	0.27	**0.74**	0.53	−0.10	−0.34
SO_4^{2-}	0.38	−0.49	−0.32	−0.49	−0.04	−0.12
	0.33	−0.50	0.04	−0.34	0.17	0.04
	0.36	−0.46	−0.40	−0.65	−0.15	−0.22
phycobilin	−0.6	−0.62	−0.40	−0.47	−0.43	**−0.74**
	−0.63	−0.51	−0.32	−0.34	−0.07	−0.45
	−0.52	−0.69	−0.31	−0.6	−0.54	−0.62
chorophyll *a*	**−0.71**	**−0.73**	−0.55	**−0.73**	**−0.75**	**−0.98**
	−0.69	−0.66	−0.61	−0.57	−0.44	−0.65
	−0.65	**−0.76**	−0.34	**−0.86**	**−0.76**	**0.77**
chorophyll *b*	−0.66	−0.64	−0.57	**−0.73**	**−0.70**	**−0.95**
	−0.63	−0.59	−0.62	−0.55	−0.41	−0.63
	−0.61	−0.66	−0.35	**−0.88**	**−0.72**	**−0.75**
chorophyll *c*	−0.52	−0.57	−0.52	−0.63	**−0.72**	**−0.92**
	−0.53	−0.5	−0.58	−0.49	−0.39	−0.66
	−0.47	−0.6	−0.32	**−0.74**	**−0.75**	−0.68

[a]Top, middle, and bottom values are for total Fe, Fe(II), and Fe(III), respectively. The bold numbers are indicated for $r > \pm 0.70$.

https://doi.org/10.1021/acs.est.0c07374
Environ. Sci. Technol. 2021, 55, 10672−10683

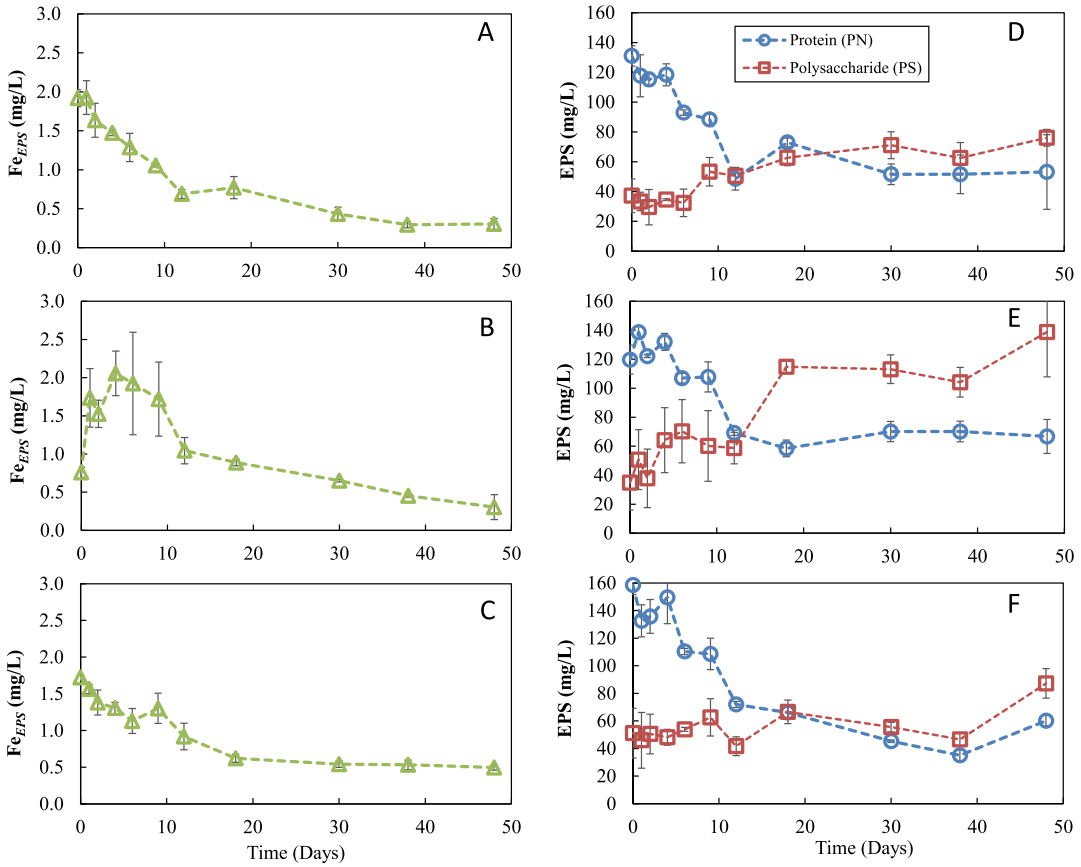

Figure 5. Fate of Fe linked with EPS (Fe_{EPS}) and EPS in hydrostatic cultivation of photogranules. Fe_{EPS} in (A) Amherst, (B) Hadley, and (C) Springfield cultivation sets. EPS-proteins and EPS-polysaccharides in (D) Amherst, (E) Hadley, and (F) Springfield cultivation sets. Error bars represent the standard deviation of triplicate samples.

Fe_{BL}, especially dissolved Fe, showed moderate to strong negative correlations with chlorophyll *a*, chlorophyll *b*, and chlorophyll *c* (Table 1). Correlations between Fe_{BL} and phycobilin were also negative but considerably weaker than with chlorophylls *b* and *c*. Consistently, the total Fe_{BL}, the sum of dissolved Fe and colloidal Fe (not shown in Table 1), mostly exhibited stronger negative correlations with chlorophyll *b* (Amherst, $r = -0.68$; Hadley, $r = -0.72$; and Springfield, $r = -0.82$) and chlorophyll *c* (Amherst, $r = -0.56$; Hadley, $r = -0.64$; and Springfield, $r = -0.82$) compared to phycobilin (Amherst, $r = -0.63$; Hadley, $r = -0.49$; and Springfield, $r = -0.55$). These results tend to indicate higher reliance of microalgae on bulk-liquid Fe for growth as compared to cyanobacteria.

Fate of Iron Linked with EPS and Its Association with Phototrophic Growth. All three cultivations progressed with significant decreases in Fe linked with EPS (Fe_{EPS}) (Figure 5A–C), indicating that the pool of Fe present in EPS underwent significant changes in cultivation. The Amherst, Hadley (from day 4), and Springfield cultivations showed the decrease in Fe_{EPS}, which could be described as a second-order decay. The second-order reaction rate constant *k* for Amherst, Springfield, and Hadley cultivations was 0.064 L/mg d (R^2 = 0.96), 0.059 L/mg d (R^2 = 0.95), and 0.033 L/mg d (R^2 = 0.92), respectively (Figure S4).

Protein in EPS (EPS-PN) showed very similar trend to Fe_{EPS} (Figure 5D–F). Indeed, strong positive correlations were found between Fe_{EPS} and EPS-PN (Amherst, $r = 0.96$; Hadley, $r = 0.76$; and Springfield, $r = 0.95$) (Table 2). By the end of cultivation, total EPS-PN was decreased by, on average, 58 ± 5%. In contrast to protein, polysaccharide in EPS (EPS-PS) showed a gradual increase from 37 ± 11 to 76 ± 6 mg/L in Amherst, 35 ± 19 to 139 ± 31 mg/L in Hadley, and 51 ± 18 to 87 ± 11 mg/L in Springfield by the end of cultivation (Figure 5D–F). These results are consistent with Kuo-Dahab et al.[27] who reported that the progression of photogranulation is accompanied with decrease in EPS-PN but increase in EPS-PS. These results also indicate that the pool of Fe linked with initial EPS in AS was utilized for photogranulation and became less available as the cultivation continued.

Table 2. Pearson Correlation Coefficients of Fe Linked with EPS (Fe_{EPS}) with Different EPS Components and Photosynthetic Pigments Produced During the Progression of Photogranulation[a]

		Amherst	Hadley	Springfield
EPS fractions	EPS-PN	**0.96**	**0.76**	**0.95**
	EPS-PS	**−0.90**	−0.63	−0.45
	EPS-PS/PN	**−0.95**	**−0.73**	**−0.93**
pigments	phycobilin	**−0.92**	**−0.76**	**−0.86**
	chlorophyll a	**−0.96**	**−0.77**	**−0.90**
	chlorophyll b	**−0.83**	−0.67	**−0.87**
	chlorophyll c	**−0.74**	−0.38	**−0.82**

[a]The bold numbers are indicated for $r > \pm 0.70$.

There were strong negative correlations between the levels of Fe_{EPS} and photosynthetic pigments in the biomass (Table 2). The degree of correlations among different pigments

https://doi.org/10.1021/acs.est.0c07374
Environ. Sci. Technol. 2021, 55, 10672−10683

showed similar pattern across the three cultivation sets: chlorophyll *a* > phycobilin > chlorophyll *b* > chlorophyll *c*. Among these pigments, phycobilin showed much stronger correlation with Fe_{EPS} than Fe_{BL}: Amherst (−0.92 vs −0.63), Hadley (−0.76 vs −0.49), and Springfield (−0.86 vs −0.55). These findings demonstrate that the growth of cyanobacteria was more influenced by Fe_{EPS} than Fe_{BL}, the latter of which showed greater influence on microalgae (Tables 1 and 2).

Distribution of Iron in Photogranules. Measurements of Fe in bulk liquid, EPS, and the whole biomass allowed for determining the distribution of Fe in biomass during photogranulation (Figure S5). The total Fe in the AS inoculums was 20.3 ± 3.7 mg/L (14.4 ± 2.0 mg/g), 24.4 ± 2.4 mg/L (8.2 ± 1.3 mg/g), and 32.4 ± 2.3 mg/L (14.4 ± 1.6 mg/g) for Amherst, Hadley, and Springfield, respectively. In these inoculums, the majority of Fe was present in biomass' pellet (Amherst, 91%; Hadley, 96%; and Springfield, 93%) followed by EPS extract (Amherst, 8%; Hadley, 3%; and Springfield, 5%) and bulk liquid (Amherst, 1%; Hadley, 1%; and Springfield, 2%). In all cultivations, the fraction of Fe_{EPS} decreased to, on average, 1.3 ± 0.2%, while the fraction of Fe_{pellet} increased to 97.9 ± 0.1%. In contrast, Fe_{BL} showed an increase till day 2 to 5.2 ± 1.9% and later decrease to 0.8 ± 0.2%. These results therefore indicate that the formation of OPGs occurred with the change in the distribution of Fe, primarily from extractable Fe_{EPS} to the pelletized Fe fraction. The Fe_{pellet} fraction is expected to contain intracellular Fe, unextracted Fe_{EPS}, and Fe precipitates (predominantly ferric oxyhydroxides), which are formed under oxic, circumneutral pH environments.

Speciation of Iron in the Biomass. We used multiple spectroscopic techniques to investigate the presence of possible Fe precipitates/minerals in AS inoculum and the formed photogranular biomass. In EPR spectroscopy (Figure 6), the characteristic broad peak at 160 mT, which corresponded to a *g*-value = 4.2, belongs to paramagnetic high-spin iron states (Fe^{3+}, $S = 5/2$),[52] indicating the presence of ferric oxides (Fe_xO_y). Amherst and Springfield OPGs showed a slight increase in EPR intensity, as compared to their inoculums, whereas Hadley showed no difference between the inoculum and OPG. These observations imply that ferric oxides in AS did not undergo dissociation by the photogranulation process. Furthermore, a relative increase in OPG-associated EPR peaks in Amherst and Springfield sets might suggest the formation of some new ferric oxides. It should be noted that drying of biomass for EPR analysis could have converted the present ferric oxyhydroxides/hydroxides into ferric oxides. Therefore, the generated EPR spectra are potentially a combination of ferric oxyhydroxide, hydroxide, and oxides.

To probe the phase crystallinity of present ferric oxides, we employed PXRD measurements (Figure S6). The PXRD spectra seemed to suggest the presence of crystalline forms, such as hematite, goethite, and magnetite; however, we did not find a complete diffraction pattern for any of these ferric oxides in both AS and OPG samples. Furthermore, many oxides have overlapping diffraction patterns, which presents a challenge in PXRD analysis without proper standards. The only conclusive statement we could make from PXRD patterns is that most of ferric oxides existed in the amorphous form in both AS inoculums and the formed OPGs.

FTIR analysis (Figure S7) depicted O−H broad stretching peak centered at 3300 cm^{-1} (peak 1), which potentially

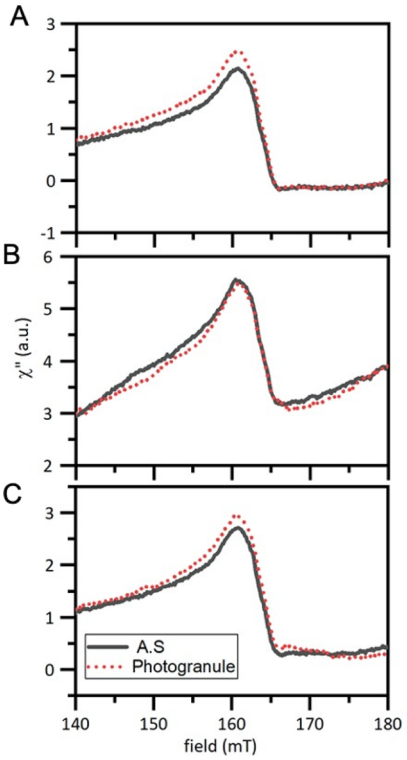

Figure 6. Room-temperature EPR spectra of AS and OPG (photogranule) in hydrostatic cultivations of (A) Amherst, (B) Hadley, and (C) Springfield sets.

suggests the presence of ferric oxyhydroxide Fe(O)OH and/or ferric hydroxides $Fe(OH)_3$ in both AS and OPGs. The progression of OPG occurred, after initial anaerobic conditions, in oxic (Figure 4C) and circumneutral pH environments, which is known to favor the formation of insoluble ferric hydroxides. Swanner et al.[53] stated that cyanobacterium *Synechococcus* oxidized Fe(II) to ferric oxyhydroxide via chemical oxidation using photosynthetic oxygenation. The O−H group stretches can also potentially belong to the carboxylic group of polysaccharides. Cyanobacteria have been reported to accumulate Fe precipitates on their outer polysaccharide sheath.[54,55] Besides polysaccharide, FTIR spectra also depicted potential interactions between Fe(III) and protein due to the presence of amide carbonyl, amide II, and carboxylic groups[56,57] (Figure S7). These FTIR results, along with literature findings and correlations between EPS fractions and Fe (Table 2), might indicate possible complexation between Fe(III) and EPS fractions (PN and PS).

DISCUSSION

The present study aimed to understand the impact of the availability of Fe on conversion of AS into OPGs, which occurs in a hydrostatic environment with a source of light. As the main approach, we chose to investigate and describe the fate of Fe in this hydrostatic photogranulation process, which has remained veiled until this study.

In AS inoculums, Fe present in bulk liquids was less than 2% of the total Fe. This Fe_{BL}, comprising dissolved and colloidal Fe, increased significantly as the hydrostatic cultivation was initiated (Figures 3 and 4). This sharp Fe release was observed to occur simultaneously with the decrease in Fe_{EPS} and EPS-

https://doi.org/10.1021/acs.est.0c07374
Environ. Sci. Technol. 2021, 55, 10672−10683

PN, and the decreases of these two AS components became more pronounced as the cultivation continued (Figure 5).

At the peak release of Fe, 42 ± 10% of Fe_{BL} was found as Fe(II). As all ASs were collected from the aeration basin and showed DO at the beginning of cultivation, the release of Fe(II) along with the decreases in Fe_{EPS} and EPS-PN reflects the reduction and solubilization of Fe and associated sludge decay. This observation is congruent with earlier postulations that Fe(III) has affinity for protein in AS EPS,[48−51] and that this Fe(III)-linked protein is released (and degraded) in anaerobic digestion as Fe(III) is reduced to Fe(II).[48,50] The reduction of Fe during this early cultivation period should have been caused by the development of anaerobic conditions (Figure 4) and also by photochemical Fe reduction. Although the latter was not directly covered in the current study, our later study showed that higher light intensity has greater Fe reduction potential compared to lower light intensity.[58] The same study also showed that when ferrozine, a strong Fe(II) chelator, was included in hydrostatic cultivation, Fe(II) in bulk liquids was up to eight times higher than that without ferrozine, implying that the amount of Fe(II) released could have been far greater than what was observed in the current study. This suggests, and it is well known from the literature,[59,60] that Fe(II) in the aquatic environment is highly labile, susceptible to and undergoing various abiotic and biotic reactions.

With the presence of light energy, the released Fe and increased PO_4^{3-}, NH_4^+, DOC, and DON (Figures 2 and S3) should have caused substantial changes in nutritional states of the system, transforming an initial fasting condition to a feasting condition (Gikonyo et al.[61]). Then, the following phototrophic growth was evident (Figures S1 and S2), which was accompanied by replenishment of DO (Figure 4). By day 9, DO in all cultivation sets increased above 2 mg/L. These changes were preceded by apparent decreases in Fe_{BL} (Figures 3 and 4). Analyses of microscopy (Figure S1), phototrophic pigmentation (Figure S2), and correlations between Fe_{BL} and pigments (Table 1) suggest that the main phototrophic group enriched during this period (prior to ∼12 d) is microalgae, which seems to take advantage of the early release of Fe.

After day 12, microalgae growth reached plateau, around which all dissolved and colloidal Fe(II) got removed and remained undetected till the end of cultivation (Figure 4A). The majority of bulk-liquid Fe(III) was also removed by the same period, but there was still some significant amount of both dissolved and colloidal Fe(III) remaining (Figure 4B). According to the literature, up to 99% of dissolved Fe is complexed with dissolved organic matter in aquatic environments.[10,62] Likewise, most colloidal Fe is also complexed with organic ligands.[63] If Fe(III) is strongly bound with organic ligands at a low Fe/ligand ratio, then Fe(III) needs to undergo biological and/or photochemical dissociation to unchelated Fe(II) for cells' effective uptake.[64−67] In contrast, high Fe/ligand conditions can induce rapid production of unchelated Fe(III) and Fe(II) from Fe(III)−ligand complexes.[68] In this study, the descending dissolved and colloidal Fe after a short peak period created substantially low Fe/DOC ratios in bulk liquids (data not shown). This finding and the literature made us infer that the advent of oxic conditions by algae-driven photosynthesis led to the formation of strong Fe(III)−organic complexes, which in turn affected the availability of Fe_{BL} to microalgal community. During this period, transition in dominant phototrophic community from microalgae to cyanobacteria occurred across all studied hydrostatic cultivations (Figures S1 and S2D).

Phycobilin showed weaker correlations with Fe_{BL} compared to chlorophylls *b* and *c* (Table 1) but stronger correlations with Fe_{EPS} compared to the counterparts (Table 2). These results suggest that cyanobacteria could utilize Fe bound with AS EPS (Fe_{EPS}) and grow despite the earlier algal bloom and minimal Fe_{BL} remaining. This is a quite feasible scenario considering that many cyanobacteria can utilize organic carbon and organic nitrogen from their extracellular environments[69,70] and scavenge Fe bound with these organic matter.[27,71] Strong correlations found between Fe_{EPS} and nitrogenous EPS (i.e., EPS-PN) and their correlations with phycobilin corroborate this statement. Fewer amounts of Fe_{EPS} became available as the cultivation continued. It is important to note that significant biomass contraction and granulation occurred when phycobilin and Fe_{EPS} leveled off (Amherst: days 18−30; Hadley: days 30−48; and Springfield: days 18−30) (Figures 1, 5; S2). It can be therefore inferred that the limitation of available Fe affected the growth of cyanobacteria, causing their physiology change, leading to forming a spherical aggregate.

Fe in the pellet increased from 92 to 98% by photogranulation. The VSS of AS inoculum is mainly composed of bacterial cells (with negligible amounts of phototrophic community) and EPS, with the latter constituting 50−80% of VSS.[72,73] Fe within bacterial cells (i.e., intracellular Fe) is reported to be approximately 0.2% of the dry biomass.[74] The average VSS of AS was 1109 ± 78 mg/L (Amherst), 2178 ± 181 mg/L (Hadley), and 1569 ± 91 mg/L (Springfield). If we assume that 50% of AS VSS was attributed from bacterial cells, the intracellular Fe in each inoculum would be then 1.1, 2.2, and 1.6 mg/L in Amherst, Hadley, and Springfield cultivations, respectively. This means that the majority of Fe in inoculums existed in the extracellular milieu of AS, possibly as Fe_{EPS}, adsorbed/trapped Fe minerals, and/or other ways of existence.

Congruent with previous reports,[26,27] the change in VSS concentrations during cultivation was insignificant although a substantive phototrophic growth occurred. This indicates that a significant fraction of organic carbon and nutrients in AS was turned over and recycled for phototrophic growth. Insignificant changes in VSS imply that still limited amount of Fe was present as intracellular Fe in formed OPGs. It should be, however, pointed out that cyanobacteria are reported to require five to eight times higher cellular Fe/C ratio than microalgae for growth.[75,76] Hence, it may be possible that significantly more Fe was present as intracellular Fe in OPGs compared to AS inoculums; however, even this consideration is not expected to change the order of magnitude for intracellular Fe versus extracellular Fe in OPGs.

Fe in the extracellular matrix of the formed OPGs could contain Fe precipitates/minerals and Fe bound with EPS which could not be extracted by the methods used. EPR (Figure 6) and PXRD (Figure S6) analyses revealed the presence of amorphous Fe oxides, which remained almost unchanged from the inoculums to OPGs. Insoluble Fe particulate/minerals cannot be directly acquired by microorganisms[23] and need to undergo a series of biological or photochemical dissociation processes to become available.[77−79] According to Wahid and Kamalam,[80] amorphous Fe oxides are more accessible than crystalline Fe oxides, and they can undergo reductive dissolution by bacteria under anaerobic conditions. It might be possible that an equilibrium was established between the formation and utilization of

https://doi.org/10.1021/acs.est.0c07374
Environ. Sci. Technol. 2021, 55, 10672−10683

amorphous Fe oxides, which could result in overall no change during the photogranulation process. Contrarily, it is also possible that amorphous Fe oxides in AS was not readily available for bacteria during the photogranulation process, due to the lack of feasible mechanisms. Recently, Basu et al.[24] provided evidence for symbiotic interactions between filamentous cyanobacteria *Trichodesmium* and their associated heterotrophic bacteria for the acquisition of Fe from dust. The study showed that tuft or puff form of *Trichodesmium* colonies captured dust-bound Fe and shuffled it to the colony core where bacteria resided. These bacteria aided in the dissolution of Fe by producing siderophores. The dissolved siderophore−Fe complex was later acquired by both *Trichodesmium* and their resident bacteria. Hydrostatically formed OPGs have a distinct dark, anaerobic region which contains facultative and obligate anaerobic bacterial community.[26] Bacteria can convert Fe(III) minerals to dissolved Fe(II) via reductive dissolution under dark anaerobic conditions.[81] Hence, there is a possibility that by forming a spherical aggregate, filamentous cyanobacteria can establish a mutualistic relationship with bacterial community and, thereby effectively utilize a unconventional Fe pool. This condition could encourage bacteria to make Fe accessible for cyanobacteria, in exchange for photosynthesis-induced organic matter.

Filamentous cyanobacteria can also directly scavenge Fe under Fe-limited conditions using their own siderophores. Filamentous cyanobacteria, such as *Anabaena* and *Oscillatoria*, are known to exhibit the siderophore-mediated Fe uptake mechanism.[5,17] The literature suggests that filamentous cyanobacteria aggregate to promote close proximity between their filaments and Fe particles, thereby preventing diffusive loss of siderophore−Fe complexes to the surrounding water.[24]

This study therefore reaches the conclusion that the access and utility of Fe_{EPS} selects cyanobacteria in hydrostatic cultivations, but the limitation of this Fe pool causes their physiological changes, which seems to become an important driver for the formation of granular structures. This way, filamentous cyanobacteria may access unutilized Fe particulates/minerals within a spherical aggregate. Dissolution of these Fe resources may occur over an extended length of period and can potentially explain why mature OPGs retain their morphology and function even years after their formation. Future studies are warranted to validate the cause-and-effect relationship between the development of OPGs and Fe limitation. Studies may use AS inoculum supplemented with Fe (to prevent Fe limitation) or treated with an Fe scavenger (to induce Fe limitation). Similarly, AS can also be cultivated in a defined media with different amounts of Fe to test the impact of varying Fe levels on OPG formation. We expect that studying the physiology of filamentous cyanobacteria associated with the availability of Fe under these various cultivation conditions would enhance our knowledge of photogranulation. Improved understanding of photogranulation will be useful to advance its engineering for aerobic but aeration-free wastewater treatment.

■ ASSOCIATED CONTENT

Supporting Information

The Supporting Information is available free of charge at https://pubs.acs.org/doi/10.1021/acs.est.0c07374.

Detailed materials and methods; correlations between phycobilin and other pigments; correlation between Fe and organic matter in bulk liquids; microscopy of hydrostatic cultivation; changes in phototrophic pigments in hydrostatic cultivation; changes in DOC and DON; second-order reaction of Fe_{EPS}; distribution of Fe in biomass; PXRD of biomass; and FTIR of biomass (PDF)

■ AUTHOR INFORMATION

Corresponding Author

Chul Park − *Department of Civil and Environmental Engineering, University of Massachusetts, Amherst, Amherst, Massachusetts 01003, United States;* orcid.org/0000-0003-0695-8562; Email: chulp@umass.edu

Authors

Abeera A. Ansari − *Department of Civil and Environmental Engineering, University of Massachusetts, Amherst, Amherst, Massachusetts 01003, United States; U.S.-Pakistan Center for Advanced Studies in Energy (USPCAS-E), National University of Sciences and Technology (NUST), 44000 Islamabad, Pakistan*

Arfa A. Ansari − *Department of Civil and Environmental Engineering, University of Massachusetts, Amherst, Amherst, Massachusetts 01003, United States*

Ahmed S. Abouhend − *Department of Civil and Environmental Engineering, University of Massachusetts, Amherst, Amherst, Massachusetts 01003, United States*

Joseph G. Gikonyo − *Department of Civil and Environmental Engineering, University of Massachusetts, Amherst, Amherst, Massachusetts 01003, United States;* orcid.org/0000-0001-5035-4059

Complete contact information is available at: https://pubs.acs.org/10.1021/acs.est.0c07374

Notes

The authors declare no competing financial interest.

■ ACKNOWLEDGMENTS

The authors thank Dr. Dhandapani Venkataraman and Dr. Kevin Kittilstved for providing laboratory facilities in the Department of Chemistry at UMass Amherst. The authors also thank Mohammad Abdullah and Andrew Keyser for insightful comments and suggestions during the study. This work was supported by the grants from the National Science Foundation (CBET1605424; IIP1919091) and the National University of Sciences and Technology, Pakistan.

■ REFERENCES

(1) Rueter, J. G.; Petersen, R. R. Micronutrient Effects on Cyanobacterial Growth and Physiology. *N. Z. J. Mar. Freshwater Res.* **1987**, *21*, 435−445.

(2) Fujii, M.; Dang, T. C.; Rose, A. L.; Omura, T.; Waite, T. D. Effect of Light on Iron Uptake by the Freshwater Cyanobacterium Microcystis Aeruginosa. *Environ. Sci. Technol.* **2011**, *45*, 1391−1398.

(3) Schoffman, H.; Lis, H.; Shaked, Y.; Keren, N.; Bibby, T. Iron − Nutrient Interactions within Phytoplankton. *Front. Plant Sci.* **2016**, *7*, 1223.

(4) Wilhelm, S. W..; Trick, C. G. Iron-Limited Growth of Cyanobacteria: Multiple Siderophore Production Is a Common Response. *Limnol. Oceanogr.* **1994**, *39*, 1979−1984.

(5) Rudolf, M.; Kranzler, C.; Lis, H.; Margulis, K.; Stevanovic, M.; Keren, N.; Schleiff, E. Multiple Modes of Iron Uptake by the Filamentous, Siderophore-Producing Cyanobacterium, Anabaena Sp. PCC 7120. *Mol. Microbiol.* **2015**, *97*, 577−588.

(6) Alexova, R.; Fujii, M.; Birch, D.; Cheng, J.; Waite, T. D.; Ferrari, B. C.; Neilan, B. A. Iron Uptake and Toxin Synthesis in the Bloom-Forming Microcystis Aeruginosa under Iron Limitation. *Environ. Microbiol.* **2011**, *13*, 1064−1077.
(7) Raven, J. A. Predictions of Mn and Fe Use Efficiencies of Phototrophic Growth as a Function of Light Availability for Growth and of c Assimilation Pathway. *New Phytol.* **1990**, *116*, 1−18.
(8) Brand, L. E. Minimum Iron Requirements of Marine Phytoplankton and the Implications for the Biogeochemical Control of New Production. *Limnol. Oceanogr.* **1991**, *36*, 1756−1771.
(9) Kustka, A.; Carpenter, E. J.; Sañudo-Wilhelmy, S. A. Iron and Marine Nitrogen Fixation: Progress and Future Directions. *Res. Microbiol.* **2002**, *153*, 255−262.
(10) Lis, H.; Kranzler, C.; Keren, N.; Shaked, Y. A Comparative Study of Iron Uptake Rates and Mechanisms amongst Marine and Fresh Water Cyanobacteria: Prevalence of Reductive Iron Uptake. *Life* **2015**, *5*, 841−860.
(11) Kranzler, C.; Lis, H.; Shaked, Y.; Keren, N. The Role of Reduction in Iron Uptake Processes in a Unicellular, Planktonic Cyanobacterium. *Environ. Microbiol.* **2011**, *13*, 2990−2999.
(12) Salmon, T. P.; Rose, A. L.; Neilan, B. A.; Waite, T. D. The FeL Model of Iron Acquisition: Nondissociative Reduction of Ferric Complexes in the Marine Environment. *Limnol. Oceanogr.* **2006**, *51*, 1744−1754.
(13) Reguera, G.; McCarthy, K. D.; Mehta, T.; Nicoll, J. S.; Tuominen, M. T.; Lovley, D. R. Extracellular Electron Transfer via Microbial Nanowires. *Nature* **2005**, *435*, 1098−1101.
(14) Gorby, Y. A.; Yanina, S.; McLean, J. S.; Rosso, K. M.; Moyles, D.; Dohnalkova, A.; Beveridge, T. J.; Chang, I. S.; Kim, B. H.; Kim, K. S.; Culley, D. E.; Reed, S. B.; Romine, M. F.; Saffarini, D. A.; Hill, E. A.; Shi, L.; Elias, D. A.; Kennedy, D. W.; Pinchuk, G.; Watanabe, K.; Ishii, S.; Logan, B.; Nealson, K. H.; Fredrickson, J. K. Electrically Conductive Bacterial Nanowires Produced by Shewanella Oneidensis Strain MR-1 and Other Microorganisms. *Proc. Natl. Acad. Sci. U.S.A.* **2006**, *103*, 11358−11363.
(15) Lamb, J. J.; Hill, R. E.; Eaton-rye, J. J.; Hohmann-marriott, M. F. Functional Role of PilA in Iron Acquisition in the Cyanobacterium Synechocystis Sp. PCC 6803. *PLoS One* **2014**, *9*, No. e105761.
(16) Gonzalez-Aravena, A. C.; Yunus, K.; Zhang, L.; Norling, B.; Fisher, A. C. Tapping into Cyanobacteria Electron Transfer for Higher Exoelectrogenic Activity by Imposing Iron Limited Growth. *RSC Adv.* **2018**, *8*, 20263−20274.
(17) Brown, C. M.; Trick, C. G. Response of the Cyanobacterium, Oscillatoria Tenuis, to Low Iron Environments: The Effect on Growth Rate and Evidence for Siderophore Production. *Arch. Microbiol.* **1992**, *157*, 349−354.
(18) Sonier, M. B.; Contreras, D. A.; Treble, R. G.; Weger, H. G. Two Distinct Pathways for Iron Acquisition by Iron- Limited Cyanobacterial Cells: Evidence from Experiments Using Siderophores and Synthetic Chelators. *Botany* **2012**, *90*, 181−190.
(19) Erdner, D. L.; Price, N.; Doucette, G.; Peleato, M.; Anderson, D. Characterization of Ferredoxin and Flavodoxin as Markers of Iron Limitation in Marine Phytoplankton. *Mar. Ecol.: Prog. Ser.* **1999**, *184*, 43−53.
(20) Chen, Y.-B.; Zehr, J. P.; Mellon, M. Growth and Nitrogen Fixation of the Diazotrophic Filamentous Nonheterocystous Cyanobacterium Trichodesmium Sp IMS 101 in Defined Media:Evidence for a Circadian Rhythm. *J. Phycol.* **1996**, *32*, 916−923.
(21) Bell, P. R. F.; Uwins, P. J. R.; Elmetri, I.; Phillips, J. A.; Fu, F.-X.; Yago, A. J. E. Laboratory Culture Studies of Trichodesmium Isolated from the Great Barrier Reef Lagoon, Austraila. *Hydrobiologia* **2005**, *532*, 9−21.
(22) Tzubari, Y.; Magnezi, L.; Be'er, A.; Berman-Frank, I. Iron and Phosphorus Deprivation Induce Sociality in the Marine Bloom-Forming Cyanobacterium Trichodesmium. *ISME J.* **2018**, *12*, 1682−1693.
(23) Rubin, M.; Berman-Frank, I.; Shaked, Y. Dust-and Mineral-Iron Utilization by the Marine Dinitrogen-Fixer Trichodesmium. *Nat. Geosci.* **2011**, *4*, 529−534.
(24) Basu, S.; Gledhill, M.; de Beer, D.; Prabhu Matondkar, S. G.; Shaked, Y. Colonies of Marine Cyanobacteria Trichodesmium Interact with Associated Bacteria to Acquire Iron from Dust. *Commun. Biol.* **2019**, *2*, 284.
(25) Frischkorn, K. R.; Haley, S. T.; Dyhrman, S. T. Coordinated Gene Expression between Trichodesmium and Its Microbiome over Day-Night Cycles in the North Pacific Subtropical Gyre. *ISME J.* **2018**, *12*, 997−1007.
(26) Milferstedt, K.; Kuo-Dahab, W. C.; Butler, C. S.; Hamelin, J.; Abouhend, A. S.; Stauch-White, K.; McNair, A.; Watt, C.; Carbajal-González, B. I.; Dolan, S.; Park, C. The Importance of Filamentous Cyanobacteria in the Development of Unusual Oxygenic Photogranules. *Sci. Rep.* **2017**, *7*, 17944.
(27) Kuo-Dahab, W. C.; Stauch-White, K.; Butler, C. S.; Gikonyo, G. J.; Carbajal-González, B.; Ivanova, A.; Dolan, S.; Park, C. Investigation of the Fate and Dynamics of Extracellular Polymeric Substances (EPS) during Sludge-Based Photogranulation under Hydrostatic Conditions. *Environ. Sci. Technol.* **2018**, *52*, 10462−10471.
(28) Abouhend, A. S.; McNair, A.; Kuo-Dahab, W. C.; Watt, C.; Butler, C. S.; Milferstedt, K.; Hamelin, J.; Seo, J.; Gikonyo, G. J.; El-Moselhy, K. M.; Park, C. The Oxygenic Photogranule Process for Wastewater Treatment. *Environ. Sci. Technol.* **2018**, *52*, 3503−3511.
(29) Ansari, A. A.; Abouhend, A. S.; Park, C. Effects of Seeding Density on Photogranulation and the Start-up of the Oxygenic Photogranule Process for Aeration-Free Wastewater Treatment. *Algal Res.* **2019**, *40*, 101495.
(30) Stauch-White, K.; Srinivasan, V. N.; Camilla Kuo-Dahab, W.; Park, C.; Butler, C. S. The Role of Inorganic Nitrogen in Successful Formation of Granular Biofilms for Wastewater Treatment That Support Cyanobacteria and Bacteria. *AMB Express* **2017**, *7*, 146.
(31) Castenholz, R. W.; Rippka, R.; Herdman, M.; Wilmotte, A. *Bergey's Manual of Systematics of Archaea and Bacteria*; John Wiley & Sons, Ltd, 2015.
(32) De Baar, H. J. W.; DeJong, J. T. M.. *The Biogeochemistry of Iron in Seawater*; Turner, D. R., Hunter, K. A., Eds.; Wiley: Chichester, U.K., 2001.
(33) Park, C.; Novak, J. T. Characterization of Activated Sludge Exocellular Polymers Using Several Cation-Associated Extraction Methods. *Water Res.* **2007**, *41*, 1679−1688.
(34) APHA. *Standard Methods for the Examination of Water and Wastewater Part 4000 INORGANIC NONMETALLIC CONSTITUENTS Standard Methods for the Examination of Water and Wastewater*; American Public Health Association: New York, NY, 1999.
(35) Pierson, B. K.; Parenteau, M. N.; Griffin, B. M. Phototrophs in High-Iron-Concentration Microbial Mats: Physiological Ecology of Phototrophs in an Iron-Depositing Hot Spring. *Appl. Environ. Microbiol.* **1999**, *65*, 5474−5483.
(36) APHA. *Standard Methods for the Examination of Water and Wastewater*, 22nd ed.; Eaton, A. D., Ed.; American Public Health Association: Washington D.C., USA, 2012.
(37) Bennett, A.; Bogorad, L. Complementary Chromatic Adaptation in a Filamentous Blue-Green Alga. *J. Cell Biol.* **1973**, *58*, 419−435.
(38) Islam, M. A.; Beardall, J. Growth and Photosynthetic Characteristics of Toxic and Non-Toxic Strains of the Cyanobacteria Microcystis Aeruginosa and Anabaena Circinalis in Relation to Light. *Microorganisms* **2017**, *5*, 45.
(39) Lauceri, R.; Bresciani, M.; Lami, A.; Morabito, G. Chlorophyll a Interference in Phycocyanin and Allophycocyanin Spectrophotometric Quantification. *J. Limnol.* **2017**, *77*, 169.
(40) DuBois, M.; Gilles, K. A.; Hamilton, J. K.; Rebers, P. A.; Smith, F. Colorimetric Method for Determination of Sugars and Related Substances. *Anal. Chem.* **1956**, *28*, 350−356.
(41) Caccavo, F.; Frolund, B.; Nielsen, P. H.; Nielsen, P. H. Deflocculation of Activated Sludge by the Dissimilatory Fe(III)-Reducing Bacterium Shewanella Alga BrY. *Appl. Environ. Microbiol.* **1996**, *62*, 1487−1490.
(42) Ivanikova, N. V. Lake Superior Phototrophic Picoplankton: Nitrate Assimilation Measured with a Cyanobacterial Nitrate-

https://doi.org/10.1021/acs.est.0c07374
Environ. Sci. Technol. 2021, 55, 10672−10683

Responsive Bioreporter and Genetic Diversity of the Natural Community. Ph.D. Dissertation, Bowling Green State University, 2006.
(43) Roy, S.; Llewellyn, C. A.; Egeland, E. S.; Johnsen, G. *Phytoplankton Pigments: Characterization, Chemotaxonomy and Applications in Oceanography*; Cambridge University Press, 2011.
(44) Schlüter, L.; Møhlenberg, F.; Havskum, H.; Larsen, S. The Use of Phytoplankton Pigments for Identifying and Quantifying Phytoplankton Groups in Coastal Areas:Testing the Influence of Light and Nutrients on Pigment/Chlorophyll a Ratios. *Mar. Ecol.: Prog. Ser.* **2000**, *192*, 49.
(45) Coupel, P.; Matsuoka, A.; Ruiz-Pino, D.; Gosselin, M.; Marie, D.; Tremblay, J.-É.; Babin, M. Pigment Signatures of Phytoplankton Communities in the Beaufort Sea. *Biogeosciences* **2015**, *12*, 991−1006.
(46) Molot, L. A.; Watson, S. B.; Creed, I. F.; Trick, C. G.; McCabe, S. K.; Verschoor, M. J.; Sorichetti, R. J.; Powe, C.; Venkiteswaran, J. J.; Schiff, S. L. A Novel Model for Cyanobacteria Bloom Formation: The Critical Role of Anoxia and Ferrous Iron. *Freshw. Biol.* **2014**, *59*, 1323−1340.
(47) Geißler, F.; Achterberg, E. P.; Beaton, A. D.; Hopwood, M. J.; Clarke, J. S.; Mutzberg, A.; Mowlem, M. C.; Connelly, D. P.; Rose, A. Evaluation of a Ferrozine Based Autonomous in Situ Lab-on-Chip Analyzer for Dissolved Iron Species in Coastal Waters. *Front. Mar. Sci.* **2017**, *4*, 00322.
(48) Park, C.; Abu-Orf, M. M.; Novak, J. T. The Digestibility of Waste Activated Sludges. *Water Environ. Res.* **2006**, *78*, 59−68.
(49) Park, C.; Muller, C. D.; Abu-Orf, M. M.; Novak, J. T. The Effect of Wastewater Cations on Activated Sludge Characteristics: Effects of Aluminum and Iron in Floc. *Water Environ. Res.* **2006**, *78*, 31−40.
(50) Park, C.; Helm, R. F.; Novak, J. T. Investigating the Fate of Activated Sludge Exocelluar Proteins in Sludge Digestion Using Sodium Dodecyl Sulfate Polyacrylamide Gel Electrophoresis (SDS-PAGE). *Water Environ. Res.* **2008**, *80*, 2219−2227.
(51) Park, C.; Novak, J. T.; Helm, R. F.; Ahn, Y.-O.; Esen, A. Evaluation of the Extracellular Proteins in Full-Scale Activated Sludges. *Water Res.* **2008**, *42*, 3879−3889.
(52) Kumar, P.; Bulk, M.; Webb, A.; van der Weerd, L.; Oosterkamp, T. H.; Huber, M.; Bossoni, L. A Novel Approach to Quantify Different Iron Forms in Ex-Vivo Human Brain Tissue. *Sci. Rep.* **2016**, *6*, 38916.
(53) Swanner, E. D.; Wu, W.; Hao, L.; Wustner, M. L.; Obst, M.; Moran, D. M.; Mcllvin, M. R.; Saito, M. A.; Kappler, A. Physiology, Fe(II) Oxidation, and Fe Mineral Formation by a Marine Planktonic Cyanobacterium Grown under Ferruginous Conditions. *Front. Earth Sci.* **2015**, *3*, 60.
(54) Bender, J.; Rodriguez-Eaton, S.; Ekanemesang, U. M.; Phillips, P. Characterization of Metal-Binding Bioflocculants Produced by the Cyanobacterial Component of Mixed Microbial Mats. *Appl. Environ. Microbiol.* **1994**, *60*, 2311−2315.
(55) *Ecology of Cyanobacteria II: Their Diversity in Space and Time*; Whitton, B. A., Ed.; Springer: Durham, U.K., 2012.
(56) Smith, B. C. *Infrared Spectral Interpretation: A Systematic Approach*; Taylor & Francis, 1998.
(57) Kong, J.; Yu, S. Fourier Transform Infrared Spectroscopic Analysis of Protein Secondary Structures. *Acta Biochim. Biophys. Sin.* **2007**, *39*, 549−559.
(58) Ansari, A. A. Investigating the Role of Iron in the Photogranulation Phenomenon. Ph.D. Dissertation, University of Massachusetts, Amherst, USA, 2020.
(59) Sunda, W. G. Bioavailability and Bioaccumulation of Iron in the Sea. In *The Biogeochemistry of Iron in Seawater*; Turner, D., Hunter, K., Eds.; John Wiley & Sons: Chichester, U.K., 2001; pp 41−84.
(60) Rose, A. L.; Waite, T. D. Effect Ofdissolved Natural Organic Matter Onthe Kinetics Offerrous Iron Oxygenation in Seawater. *Environ. Sci. Technol.* **2003**, *37*, 4877−4886.
(61) Gikonyo, J. G.; Ansari, A. A.; Abouhend, A.; Tobiason, J. E.; Park, C. Hydrodynamic Granulation of Oxygenic Photogranules. *Environ. Sci.: Water Res. Technol.* **2021**, *7*, 427−440.
(62) Wu, J.; Luther, G. W. Complexation of Fe(III) by Natural Organic Ligands in the Northwest Atlantic Ocean by a Competitive Ligand Equilibration Method and a Kinetic Approach. *Mar. Chem.* **1995**, *50*, 159−177.
(63) von der Heyden, B. P.; Roychoudhury, A. N. A Review of Colloidal Iron Partitioning and Distribution in the Open Ocean. *Mar. Chem.* **2015**, *177*, 9−19.
(64) Barbeau, K.; Rue, E. L.; Bruland, K. W.; Butler, A. Photochemical Cycling of Iron in the Surface Ocean Mediated by Microbial Iron (III)-Binding Ligands. *Nature* **2001**, *413*, 409−413.
(65) Fujii, M.; Rose, A. L.; Omura, T.; Waite, T. D. Effect of Fe(II) and Fe(III) Transformation Kinetics on Iron Acquisition by a Toxic Strain of Microcystis Aeruginosa. *Environ. Sci. Technol.* **2010**, *44*, 1980−1986.
(66) Fujii, M.; Dang, T. C.; Bligh, M. W.; Rose, A. L.; Waite, T. D. Effect of Natural Organic Matter on Iron Uptake by the Freshwater Cyanobacterium Microcystis Aeruginosa. *Environ. Sci. Technol.* **2014**, *48*, 365−374.
(67) Fu, Q.-L.; Fujii, M.; Natsuike, M.; Waite, T. D. Iron Uptake by Bloom-Forming Freshwater Cyanobacterium Microcystis Aeruginosa in Natural and Effluent Waters. *Environ. Pollut.* **2019**, *247*, 392−400.
(68) Fujii, M.; Imaoka, A.; Yoshimura, C.; Waite, T. D. Effects of Molecular Composition of Natural Organic Matter on Ferric Iron Complexation at Circumneutral PH. *Environ. Sci. Technol.* **2014**, *48*, 4414−4424.
(69) Stuart, R. K.; Mayali, X.; Lee, J. Z.; Craig Everroad, R.; Hwang, M.; Bebout, B. M.; Weber, P. K.; Pett-Ridge, J.; Thelen, M. P. Cyanobacterial Reuse of Extracellular Organic Carbon in Microbial Mats. *ISME J.* **2016**, *10*, 1240−1251.
(70) Stal, L. J. *Algae and Cyanobacteria in Extreme Environments*; Seckbach, J., Ed.; Springer: Netherlands, 2007.
(71) Sorichetti, R. J.; Creed, I. F.; Trick, C. G. The Influence of Iron, Siderophores and Refractory DOM on Cyanobacterial Biomass in Oligotrophic Lakes. *Freshw. Biol.* **2014**, *59*, 1423−1436.
(72) Dignac, M.-F.; Urbain, V.; Rybacki, D.; Bruchet, A.; Snidaro, D.; Scribe, P. Chemical Description of Extracellular Polymers: Implication on Activated Sludge Floc Structure. *Water Sci. Technol.* **1998**, *38*, 45−53.
(73) Wilén, B.-M.; Jin, B.; Lant, P. The Influence of Key Chemical Constituents in Activated Sludge on Surface and Flocculating Properties. *Water Res.* **2003**, *37*, 2127−2139.
(74) Metcalf, E. *Wastewater Engineering: Treatment and Reuse*, 4th ed.; McGraw-Hill: Boston, Massachusetts, 2003.
(75) Keren, N.; Aurora, R.; Pakrasi, H. B. Critical Roles of Bacterioferritins in Iron Storage and Proliferation of Cyanobacteria. *Plant Physiol.* **2004**, *135*, 1666−1673.
(76) Allen, M. D.; del Campo, J. A.; Kropat, J.; Merchant, S. S. FEA1, FEA2, and FRE1, Encoding Two Homologous Secreted Proteins and a Candidate Ferrireductase, Are Expressed Coordinately with FOX1 and FTR1 in Iron-Deficient Chlamydomonas Reinhardtii. *Eukaryot. Cell* **2007**, *6*, 1841−1852.
(77) Sulzberger, B.; Laubscher, H. Reactivity of Various Types of Iron(III) (Hydr)Oxides towards Light-Induced Dissolution. *Mar. Chem.* **1995**, *50*, 103−115.
(78) Borer, P.; Sulzberger, B.; Hug, S. J.; Kraemer, S. M.; Kretzschmar, R. Photoreductive Dissolution of Iron(III) (Hydr)-Oxides in the Absence and Presence of Organic Ligands: Experimental Studies and Kinetic Modeling. *Environ. Sci. Technol.* **2009**, *43*, 1864−1870.
(79) Sulzberger, B.; Suter, D.; Siffert, C.; Banwart, S.; Stumm, W. Dissolution of Fe(Iii)(Hydr)Oxides in Natural Waters; Laboratory Assessment on the Kinetics Controlled by Surface Coordination. *Mar. Chem.* **1989**, *28*, 127−144.
(80) Wahid, P. A.; Kamalam, N. V. Reductive Dissolution of Crystalline and Amorphous Fe(III) Oxides by Microorganisms in Submerged Soil. *Biol. Fertil. Soils* **1993**, *15*, 144−148.
(81) Balzano, S.; Statham, P.; Pancost, R.; Lloyd, J. Role of Microbial Populations in the Release of Reduced Iron to the Water

https://doi.org/10.1021/acs.est.0c07374
Environ. Sci. Technol. 2021, 55, 10672−10683

Column from Marine Aggregates. *Aquat. Microb. Ecol.* **2009**, *54*, 291−303.

https://doi.org/10.1021/acs.est.0c07374
Environ. Sci. Technol. 2021, 55, 10672−10683